Energy Efficiency Analysis of an Electric Furnace through the Implementation of a Forced Convection Fan

Análisis de la Eficiencia Energética en un Horno Eléctrico con la Implementación de un Ventilador Convectivo

I. Simbaña[1] 0000-0002-3324-3071 S. Mena[1] 0009-0005-7326-1118
S. Chasipanta[1] 0009-0002-9837-079X

[1]Instituto Superior Universitario Sucre, Grupo de Investigación en Ingeniería Mecánica y Pedagogía de la Carrera de Electromecánica (GIIMPCEM), Quito, Ecuador
E-mail: isimbana@tecnologicosucre.edu.ec, sarai.13.mena@gmail.com, silvanabigail.12@gmail.com

Abstract

This study presents an energy efficiency analysis of an electric furnace used for tempering heat treatments by implementing a forced convection fan. Improving energy efficiency in industrial heating systems remains a critical challenge, driven by the need to lower operational costs and enhance sustainability. A numerical model was developed based on heat transfer mechanisms, applying computational fluid dynamics (CFD) with a mesh of 138 565 elements and a validated mesh quality factor of 4.681. The continuity, momentum, and energy conservation equations were analyzed under real operating conditions. Results indicated that the maximum temperature increased from 290 to 327.2 K with the addition of the fan, while electrical consumption rose by only 1.54%, corresponding to an additional cost of merely USD 0.0005 per operating cycle. This thermal enhancement promotes greater temperature uniformity and reduces operational times. Consequently, integrating a forced convection system in industrial electric furnaces proves to be a technically and economically viable strategy.

Index terms— Energy efficiency, Electric furnace, Simulation, Convective fan, CAD.

Resumen

Este trabajo presenta un análisis de eficiencia energética de un horno eléctrico utilizado para tratamiento térmico de revenido, mediante la implementación de un ventilador de convección forzada. La eficiencia energética en sistemas de calentamiento industrial es un desafío actual, impulsado por la necesidad de reducir costos operativos y mejorar la sostenibilidad. Basándose en los mecanismos de transferencia de calor, se desarrolló un modelo numérico utilizando dinámica de fluidos computacional (CFD, por sus siglas en inglés) con un mallado de 138 565 elementos y validación de calidad de malla de 4.681. Se analizaron las ecuaciones de conservación de continuidad, momento y energía, bajo condiciones reales de operación. Los resultados mostraron que la temperatura máxima alcanzada se incrementó de 290 a 327.2 K con el ventilador, mientras el consumo eléctrico aumentó solo un 1.54 %, representando un costo adicional mínimo de USD 0.0005 por ciclo de operación. Esta mejora térmica permite una mayor homogeneidad de temperatura y tiempos de operación más cortos. Por lo que, la incorporación de un sistema de convección forzada en hornos eléctricos industriales es una estrategia de alta viabilidad técnica y económica.

Palabras clave— Eficiencia energética, Horno eléctrico, Simulación, Ventilador convectivo, CAD.

Recibido: 28-04-2025, Aprobado tras revisión: 04-07-2025
Forma sugerida de citación: Simbaña, I.; Mena, S.; Chasipanta, S. (2025). "Energy Efficiency Analysis of an Electric Furnace through the Implementation of a Forced Convection Fan". Revista Técnica ***"energía"***. No. 22, Issue I, Pp. 46-52.
ISSN On-line: 2602-8492 - ISSN Impreso: 1390-5074
Doi: https://doi.org/10.37116/revistaenergia.v21.n2.2025.708

1. INTRODUCTION

Energy efficiency has become a key priority in designing and optimizing thermal systems, particularly in continuously used equipment such as electric furnaces for heat treatment. The primary driver for reducing heating time is energy savings, contributing to increased productivity and reduced operational costs. Understanding the internal flow dynamics of these systems is essential, as it directly affects thermal efficiency, potentially leading to prolonged and inefficient usage in some cases.

In this context, computer-aided design (CAD) tools and computational numerical analysis emerge as strategic tools in modern engineering. These tools enable the prediction of component behavior before manufacturing, allowing for design improvements. Specialized software is essential for three-dimensional modeling and airflow analysis within the heating chamber. Proper implementation of these systems allows for the analysis of thermal distribution in furnaces used for tempering, leading to optimized heating processes and significant reductions in electricity consumption, ultimately fostering a more sustainable and efficient industrial system.

To better understand the behavior of airflow in forced convection heating systems, the work of Loksupapaiboon et al. [1] is analyzed. They utilize computational fluid dynamics (CFD) simulations using OpenFOAM software with the SST k-ω turbulence model to analyze heat transfer in a rotating hand-shaped mold. They observe Reynolds numbers ranging from 1 583 to 15 837 and rotation rates from 0 to 5, finding significant variations in the Nusselt number based on geometry and flow conditions. The results are experimentally validated with an error of less than 7.61 %, enabling the development of predictive equations with an average error of 7.32 % and an R^2 of 0.90. The study underscores the value of simulation tools like CAD and CFD in optimizing industrial thermal processes, particularly in designing efficient forced convection systems that reduce testing times and improve heat flow management.

In the same area, Suvanjumrat and Loksupapaiboon [2] present research that uses CFD simulations with OpenFOAM to improve thermal distribution within a drying oven for rubber glove molds. By using a 3D model and the k-ε turbulence model, the study analyzes the flow of hot air through the duct grids under the conveyor chain. The research highlights that the conventional design fails to provide uniform temperature distribution, and the placement of air return channels on the side walls has a negative impact. The proposed solution is to modify the design of the hot air outlet grids, leading to improved thermal control at a low cost. The CFD model shows a significant improvement, with an average error of less than 8.99 % compared to experimental measurements, confirming the method's accuracy and applicability.

The study by Palacio-Caro et al. [3] presents a numerical simulation to assess the thermal and flow behavior in an electric tempering furnace for steel, focusing on how fan speed affects thermal efficiency, temperature homogeneity, and heat transfer to the load. The simulation tests four fan speeds, 720, 990, 1350, and 1800 rpm, and found that higher speeds improve thermal homogeneity due to increased recirculation and mixing of the airflow, which enhances heat transfer. However, this results in a 20% decrease in thermal efficiency due to higher fan energy consumption. Despite this, the heat transfer rate improves by up to 50 %, allowing for shorter heat treatment times. This simulation supports optimizing furnace operation by balancing efficiency with processing speed.

Balli et al. [4] conduct an experimental study and numerical modeling of the thermal behavior of an industrial ceramic kiln prototype, aiming to optimize energy efficiency and reduce fuel consumption and CO_2 emissions. A simplified mathematical model is developed to accurately predict the spatial and temporal temperature distribution within the kiln, enabling better control over the cooking process and ensuring the quality of the final product. The results demonstrate that this efficient technology allows for an 83 % energy savings and an 87.36 % reduction in CO_2 emissions compared to traditional kilns. The model's validation with experimental data confirms its effectiveness in optimizing thermal processes in ceramic production and suggests its broader application for other materials, promoting more sustainable manufacturing practices.

Sobottka et al. [5] introduce a production planning and control methodology based on hybrid simulation and multi-criteria optimization, applied to heat treatment in a metal foundry in Austria. By utilizing real system data and digital tools, the approach achieves a 10 % overall optimization and a 6 % energy savings. This solution, based on heuristic and genetic algorithms, enables the replacement of manual planning with more efficient results in less time. Additionally, it demonstrates the feasibility of integrating variable energy prices to align industrial energy demand with available supply. The study highlights the significant potential of digital tools in modern manufacturing and emphasizes the importance of accurate data for their successful implementation.

Knoll et al. [6] assess the impact of various turbulence models on predicting the contact between particles and walls in industrial furnaces used for particle heat treatment. The study involves transient multiphase flow numerical simulations and experimental comparisons, analyzing three approaches: RANS models (RLZ-k-ε), Reynolds stress models, and large eddy simulations (LES). The results demonstrate that LES significantly improves the accuracy in predicting the number of particles adhering to furnace walls, a crucial factor in preventing material loss. Moreover, LES simulation time was reduced to one week using RANS grids without sacrificing accuracy. This research enables better predictions of particle behavior within the furnace and more precise estimates of material loss, contributing to the efficient design of industrial furnaces through advanced simulations.

Therefore, this research aims to analyze the feasibility of adding a fan to a tempering furnace to accelerate heat distribution, thereby reaching the desired temperature more quickly. It also considers the current electricity consumption and the additional cost of implementing this new system. The paper is organized as follows: the Materials and Methods section outlines the mathematical models supporting the computational analysis, including the initial modeling stages and conditions. The Results section presents the analysis of graphs generated for the variables considered, comparing the obtained values with available literature to validate the proposal. Finally, the Conclusions section synthesizes the most relevant findings and discusses the authors' perspectives throughout the research process.

2. MATERIALS AND METHODS

2.1 Heat Transfer Mechanisms

Conduction occurs within a solid body or between bodies in direct contact, without macroscopic movement of the material. Heat flows from regions of higher temperature to lower temperature due to the thermal agitation of particles. This process follows Fourier's Law, which states that the rate of heat transfer by conduction $(\dot{Q}_{cond})$ is proportional to the temperature gradient (*dT/dx*) and the material's thermal conductivity (*k*) [7], as expressed in equation (1):

$$\dot{Q}_{cond} = -k \cdot A \cdot \frac{dT}{dx} \tag{1}$$

Where A is the cross-sectional area. Another mechanism of heat transfer is radiation, which does not require a material medium, as thermal energy is transmitted via electromagnetic waves, primarily in the infrared spectrum. All bodies with temperatures above absolute zero emit radiant heat $(\dot{Q}_{rad})$, and this phenomenon is described by the Stefan-Boltzmann Law, which states that the radiated energy per unit area of a black body is proportional to the fourth power of its absolute temperature [8], as given in equation (2):

$$\dot{Q}_{rad} = \varepsilon \cdot \sigma \cdot A \cdot (T_s^4 - T_\infty^4) \tag{2}$$

Where T_s and T_∞ represent the absolute temperatures of the surface and the surrounding environment, respectively, ε is the material's emissivity, and σ is the Stefan-Boltzmann constant. The next heat transfer mechanism is convection, which occurs when heat is transferred between a solid surface and a moving fluid, driven by both thermal conduction within the fluid and the fluid's movement. This process is governed by Newton's Law of Cooling, which relates the convective heat transfer rate $(\dot{Q}_{cond})$ to the contact area, the convective heat transfer coefficient (*h*), and the temperature difference between the fluid (T_f) and the surface [9], as shown in equation (3):

$$\dot{Q}_{conv} = h \cdot A \ (T_s - T_f) \tag{3}$$

The Nusselt number (*Nu*) is a dimensionless number that characterizes the efficiency of heat transfer by convection compared to conduction within a fluid [10] and it is defined by equation (4):

$$Nu = \frac{h \cdot L_c}{k} \tag{4}$$

Where L_c is a characteristic length. A higher Nusselt number indicates that convection dominates over conduction, with its value depending on the type of flow, geometry, and boundary conditions. Convection can be natural, where fluid movement is solely driven by density differences caused by temperature gradients. On the other hand, forced convection occurs when an external agent, such as a fan, drives the fluid movement, leading to more efficient heat exchange [11].

When forced air hits a solid surface, a complex fluid-structure interaction occurs. Upon impact, the flow changes direction sharply, creating a high-pressure zone at the front of the object and turbulence in the rear. In this rear region, as air speed decreases and vortices form, low-pressure zones emerge where heat tends to accumulate more due to the reduced drag of the fluid. Fig. 1 illustrates these pressure fluctuations, which result in more intense and variable heat transfer.

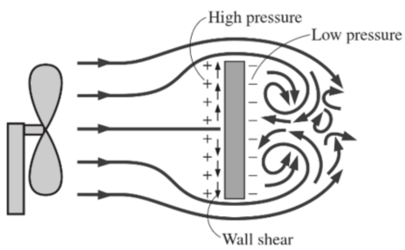

Figure 1: Pressure Fluctuations in Forced Convection [11]

2.2 Conservation Equations

The continuity equation states that mass is neither created nor destroyed within a closed system. In terms of flow, it indicates that any change in the density of a fluid within a control volume must result from the net mass flow entering or exiting the volume. The objective is to ensure that mass balance is maintained throughout the analysis of fluid dynamic systems [12], as shown in equation (5):

$$\frac{\partial u}{\partial x} + \frac{\partial v}{\partial y} = 0 \tag{5}$$

The momentum conservation equation describes how the momentum of a fluid changes due to the influence of external forces such as pressure, gravity, or friction. This equation forms the foundation of the Navier-Stokes equations, relating fluid acceleration to the applied forces, allowing the prediction of dynamic behavior [13], as expressed in equation (6):

$$\rho\left(u\frac{\partial u}{\partial x}+v\frac{\partial u}{\partial y}\right)=\mu\frac{\partial^2 u}{\partial y^2}+\frac{\partial P}{\partial x} \qquad (6)$$

The energy conservation equation establishes that the internal energy of a system can change due to heat transfer, work done by or on the system, or energy transport through the flow. This equation is crucial for modeling processes such as heating, cooling, and phase changes in thermal systems, combining Thermodynamics principles with Fluid Mechanics [14], as given in equation (7):

$$\rho\cdot C_p\left(u\frac{\partial T}{\partial x}+v\frac{\partial T}{\partial y}\right)=k\left(\frac{\partial^2 T}{\partial x^2}+\frac{\partial^2 T}{\partial y^2}\right) \qquad (7)$$

2.3 Energy Efficiency

The electrical energy (E) consumed by an equipment refers to the total amount of energy used over a specified period of operation. It is a fundamental parameter for assessing the energy consumption and economic costs of a system. It is calculated by multiplying the electrical power of the equipment (P) by the time it operates (t) [15], as shown in equation (8):

$$\frac{dE(t)}{dt}=P(t) \qquad (8)$$

Energy efficiency (η) indicates how effectively a system converts the energy consumed into useful energy, expressing the percentage of electrical energy consumed that is converted into useful heat (Q) to raise the temperature of the treated element [16], as outlined in equation (9):

$$\eta=\frac{Q}{E} \qquad (9)$$

2.4 Modeling

Fig. 2a presents the initial geometry of the furnace, emphasizing that it is constructed from stainless steel and operates using 10 mm diameter electric resistors located on the side panels. The furnace specifications indicate a power rating of 6.5 kW, requiring a two-phase 220 V power supply. Fig. 2b displays the furnace chamber dimensions, which have been established at a volume of 125 L.

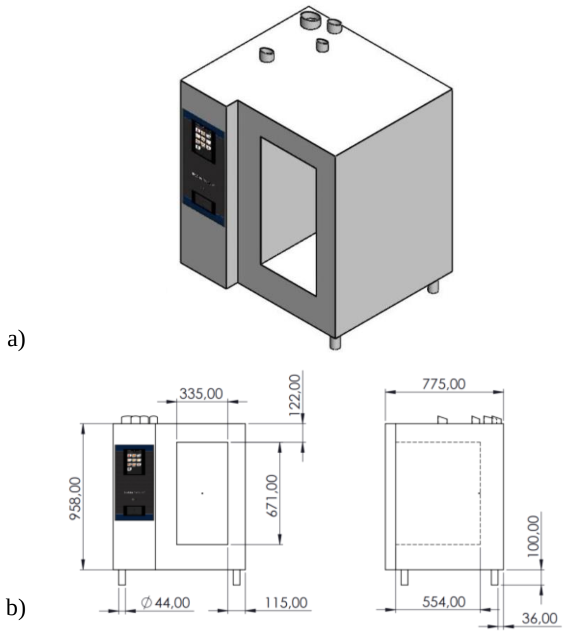

Figure 2: Electric Furnace for Tempering Thermal Treatment, a) 3D Model, b) Dimensions

Fig. 3 shows the proposed design modification, which includes integrating a fan into the rear panel of the furnace chamber. The fan was selected based on its availability in the local market and its suitability for the established temperature range. The chosen axial fan has six blades, a 250 mm diameter, is made of stainless steel, and has a maximum rotational speed of 1 400 rpm.

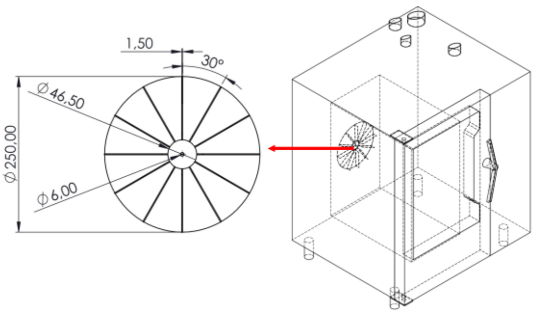

Figure 3: Geometry of the Convective Fan within the Furnace Chamber

2.5 Initial Conditions

Fig. 4a illustrates the discretization process, using dominant tetrahedra as the meshing technique. A total of 138,565 elements and 213,720 nodes were generated, and mesh quality was validated through aspect ratio analysis, which compares the generated elements to perfect symmetry, with an ideal value of zero. In this case, an aspect ratio of 4.681 was obtained, which is considered to have good quality as it is below 5 [17]. Fig. 4b shows the definition of the area to be simulated using computational fluid dynamics, with the experimental parameters setting a heat flux of 1.8 kW/m².

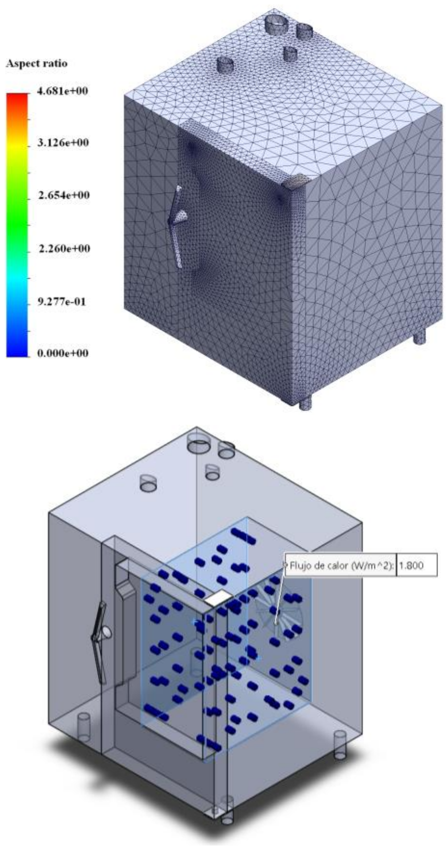

a)

b)

Figure 4: Initial Conditions, a) Meshing, b) Definition of Flow Area

3. RESULTS

Fig. 5 displays the analysis of the hot air flow velocity within the furnace chamber. With the fan's maximum rotational speed of 1 400 rpm, the maximum air velocity reached is 21.91 m/s. This ensures continuous air circulation, allowing it to reach all areas of the chamber, including the farthest corners.

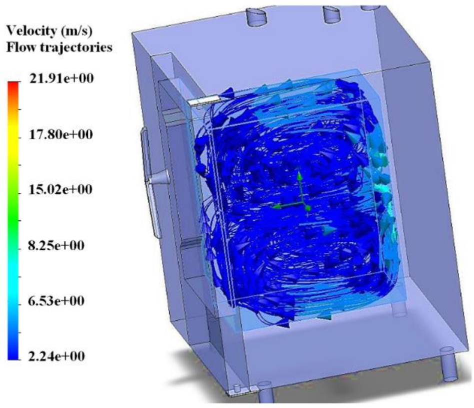

Figure 5: Airflow Velocity Analysis

Fig. 6a shows the temperature distribution inside the furnace after 150 seconds of simulation time, with 20 iterations per step and the fan turned off. Figure 6b presents the temperature simulation results under the same conditions, but with the fan turned on. Without the fan, the heat flow does not reach all areas of the furnace. However, with the fan on, the heat flow fills the interior chamber, generating forced convection. The maximum temperatures reached were 293.2 K for the furnace without ventilation and 327.2 K with the fan on.

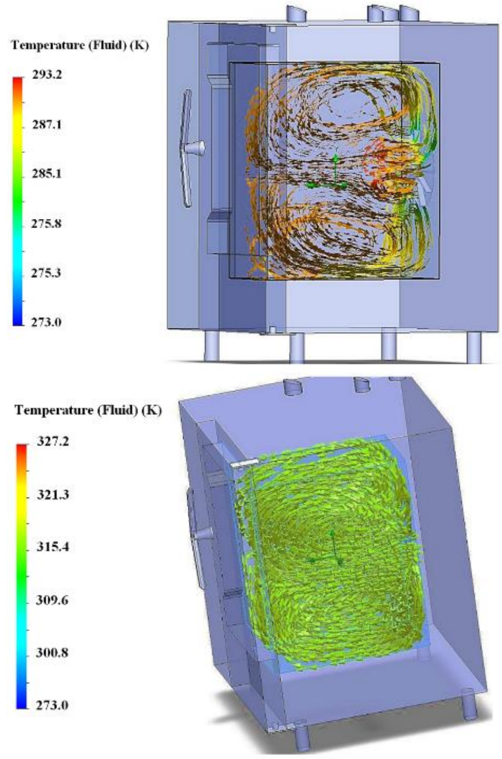

a)

b)

Figure 6: Heat Flow Inside the Furnace: a) Without Ventilation, b) With Forced Convection

Fig. 7 illustrates the temperature increase over the simulation period between the furnace without a fan and with the convective fan implementation. Additionally, experimental values measured in the furnace during a heating process over the same time frame were considered. The simulation shows a higher temperature increase due to the real losses present in the furnace. The heat flow enhances the distribution within the furnace, resulting in a temperature increase of 10.65 % compared to the initial conditions.

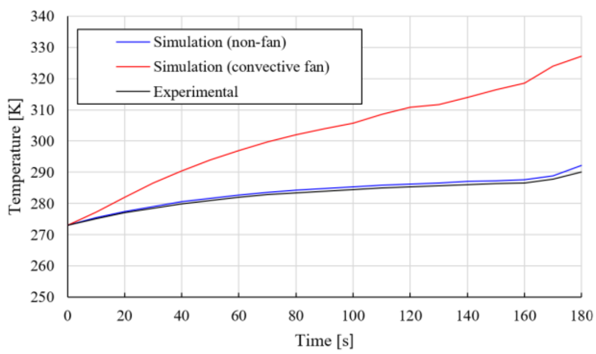

Figure 7: Comparison of Temperature Increase Under Different Simulation and Experimental Conditions

Fig. 8 compares the electrical energy consumption of the furnace in its initial condition and with the fan implementation. For energy efficiency analysis, the average electricity cost in Ecuador, approximately USD 0.10 per kW·h, was taken into account. The electrical consumption recorded for the furnace without a fan over a 180-second cycle was 0.325 kW·h, corresponding to a cost of about 0.0325 USD. With the fan, the consumption slightly increased to 0.330 kW·h, resulting in a cost of USD 0.0330. This represents a 1.54 % increase in energy consumption, which amounts to an additional USD 0.0005, a negligible difference in economic terms.

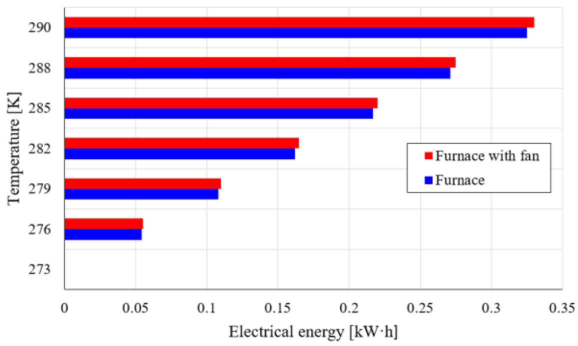

Figure 8: Electrical Energy Consumption of the Furnace in Initial Conditions and with the Convective Fan

While the thermal impact is notably positive, the simulation and experimental measurements reveal that incorporating the fan allowed for a faster temperature increase, reaching approximately 327 K compared to the 290 K of the conventional furnace within the same time frame. This indicates greater heat transfer efficiency, improved thermal homogeneity, and a potential reduction in the overall operating time for future treatment cycles. Therefore, despite the slight increase in energy consumption, the system significantly enhances productivity and could lead to notable long-term savings by reducing furnace operating times.

4. CONCLUSIONS

The energy efficiency analysis of the electric furnace through the integration of a forced convection fan has proven both feasible and advantageous. By incorporating computational fluid dynamics (CFD), the study provided valuable insights into the heat transfer mechanisms of conduction, radiation, and convection, confirming that the use of forced airflow results in a more uniform and efficient temperature distribution within the furnace chamber.

The CFD simulation demonstrated that adding a fan significantly improved the heat flux, raising the maximum temperature to 327.2 K, compared to 290 K with the conventional furnace, within the same time frame. This thermal improvement, representing a 10.65 % increase over the initial conditions, came with only a 1.54 % rise in energy consumption, translating to an additional USD 0.0005 per operating cycle, based on the cost of USD 0.10 per kW·h in Ecuador. These results highlight that the proposed solution not only enhances the thermal performance of the furnace but also maintains a low electrical consumption, contributing to both productivity and energy sustainability. Future research should focus on exploring different fan configurations, dynamic speed control, and power modulation strategies to further enhance energy efficiency and reduce operational costs in industrial heating applications for heat treatment processes.

5. REFERENCES

[1] K. Loksupapaiboon and C. Suvanjumrat, “Forced convective heat transfer and fluid flow past a rotating hand-shaped former for improving rubber glove curing,” Case Studies in Thermal Engineering, vol. 47, p. 103050, 2023. doi: 10.1016/j.csite.2023.103050

[2] C. Suvanjumrat and K. Loksupspaiboon, “Improvement of thermal distribution in the rubber-glove former conveyor oven by OpenFOAM,” Engineering Journal, vol. 24, no. 2, pp. 109–120, 2020. doi: 10.4186/ej.2020.24.2.109

[3] I. D. Palacio-Caro, P. N. Alvarado-Torres, and L. F. Cardona-Sepúlveda, “Numerical simulation of the flow and heat transfer in an electric steel tempering furnace,” Energies (Basel), vol. 13, no. 14, p. 3655, 2020.

[4] L. Balli, M. Hlimi, Y. Achenani, A. Atifi, and B. Hamri, “Experimental study and numerical modeling of the thermal behavior of an industrial prototype ceramic furnace: Energy and environmental optimization,” Energy and Built Environment, vol. 5, no. 2, pp. 244–254, 2024.

[5] T. Sobottka, F. Kamhuber, and B. Heinzl, “Simulation-based multi-criteria optimization of parallel heat treatment furnaces at a casting manufacturer,” Journal of Manufacturing and Materials Processing, vol. 4, no. 3, p. 94, 2020.

[6] M. Knoll, H. Gerhardter, C. Hochenauer, and P. Tomazic, “Influences of turbulence modeling on particle-wall contacts in numerical simulations of industrial furnaces for thermal particle treatment,” Powder Technol, vol. 373, pp. 497–509, 2020.

[7] Y. Huang, X. Xiao, H. Kang, J. Lv, R. Zeng, and J. Shen, “Thermal management of polymer electrolyte membrane fuel cells: A critical review of heat transfer mechanisms, cooling approaches, and advanced cooling techniques analysis,” Energy Convers Manag, vol. 254, p. 115221, Feb. 2022, doi: 10.1016/J.ENCONMAN.2022.115221.

[8] W. Quitiaquez, I. Simbaña, C. A. Isaza-Roldán, C. Nieto-Londoño, P. Quitiaquez, and L. Toapanta-Ramos, “Performance Analysis of a Direct-Expansion Solar-Assisted Heat Pump Using a

Photovoltaic/Thermal System for Water Heating," Communications in Computer and Information Science, vol. 1154 CCIS, pp. 89–102, 2020, doi: 10.1007/978-3-030-46785-2_8.

[9] H. Matsubara, G. Kikugawa, and T. Ohara, "Comparison of molecular heat transfer mechanisms between water and ammonia in the liquid states," International Journal of Thermal Sciences, vol. 161, p. 106762, Mar. 2021, doi: 10.1016/J.IJTHERMALSCI.2020.106762.

[10] Z. Sun, T. Wang, B. Qian, Y. Wang, J. Wang, and C. Hong, "Study on the efficient heat transfer mechanism of microchannel pin-fin arrays under low pumping power," Appl Therm Eng, vol. 241, p. 122386, Mar. 2024, doi: 10.1016/J.APPLTHERMALENG.2024.122386.

[11] H. Ma, N. Cai, L. Cai, and F. Si, "Effects of the forced convection induced by assistant fans on the thermal performance of an indirect dry cooling system," Case Studies in Thermal Engineering, vol. 35, p. 102141, Jul. 2022, doi: 10.1016/J.CSITE.2022.102141.

[12] K. Clough, "Continuity equations for general matter: applications in numerical relativity," Class Quantum Gravity, vol. 38, no. 16, p. 167001, Jul. 2021, doi: 10.1088/1361-6382/AC10EE.

[13] R. Laubscher and P. Rousseau, "Application of a mixed variable physics-informed neural network to solve the incompressible steady-state and transient mass, momentum, and energy conservation equations for flow over in-line heated tubes," Appl Soft Comput, vol. 114, p. 108050, Jan. 2022, doi: 10.1016/J.ASOC.2021.108050.

[14] I. Simbaña, W. Quitiaquez, P. Cabezas, and P. Quitiaquez, "Comparative Study of the Efficiency of Rectangular and Triangular Flat Plate Solar Collectors through Finite Element Method," Revista Técnica "Energía," vol. 20, no. 2, pp. 81–89, 2024, doi: 10.37116/revistaenergia.v20.n2.2024.593.

[15] V. Logar and I. Škrjanc, "The Influence of Electric-Arc-Furnace Input Feeds on its Electrical Energy Consumption," Journal of Sustainable Metallurgy, vol. 7, no. 3, pp. 1013–1026, Sep. 2021, doi: 10.1007/S40831-021-00390-Y/FIGURES/11.

[16] Z. Song and C. Liu, "Energy efficient design and implementation of electric machines in air transport propulsion system," Appl Energy, vol. 322, p. 119472, Sep. 2022, doi: 10.1016/J.APENERGY.2022.119472.

[17] I. Simbaña, A. Tirado, A. Arias, and X. Vaca, "Structural and kinematic analysis of the prototype of a folding work table," Novasinergia, ISSN 2631-2654, vol. 8, no. 1, pp. 19–32, Jan. 2025, doi: 10.37135/NS.01.15.08.

Isaac Simbaña. - Nació en Quito, Ecuador, en 1990. Obtuvo su título de Ingeniero Mecánico en la Universidad Politécnica Salesiana en 2018; su título de Magíster en Métodos Matemáticos y Simulación Numérica en Ingeniería y de Magíster en Educación en Universidad Politécnica Salesiana, en 2022 y 2024, respectivamente; su título de Magíster en Dirección y Administración de Empresas en la Universidad Bolivariana del Ecuador, en 2025. Actualmente cursa estudios doctorales en Ciencias. Trabaja en el Instituto Superior Universitario Sucre y es el Coordinador del Grupo de Investigación en Ingeniería Mecánica y Pedagogía de la Carrera de Electromecánica (GIIMPCEM). Sus campos de investigación están relacionados con el Análisis Numérico y Estadístico, Termodinámica, Energías, Procesos de Manufactura, Ciencia de los Materiales, así como Gestión de Operaciones e Innovación Educativa.

Saraí Mena.- Es Tecnóloga Superior en Electromecánica, graduada en el Instituto Superior Universitario Sucre en 2024. Sus intereses de investigación incluyen los procesos de manufactura, mantenimiento industrial y estructuras que involucran sueldas y uniones metálicas. Actualmente, busca ampliar sus habilidades en sistemas eléctricos automotrices y técnicas de sueldas especializadas.

Silvana Chasipanta.- Nació en Quito, en 2002. Obtuvo su título como Tecnóloga Superior en Electromecánica en el Instituto Superior Universitario Sucre en 2024. Su campo de investigación se enfoca en la Ingeniería Mecánica y la Simulación.